

Articular calcified cartilage canals in the third metacarpal bone of 2-year-old thoroughbred racehorses

A. Boyde¹ and E. C. Firth²

¹*Biophysics, Centre for Oral Growth and Development, St Barts and The London School of Medicine and Dentistry, Queen Mary, University of London, UK*

²*Institute of Veterinary, Animal and Biomedical Sciences, Massey University, New Zealand*

Abstract

We describe morphological aspects of the articular calcified cartilage mineralizing front 'tidemark' in the distal joint surface of the third metacarpal bone from 14 horses. Compositional backscattered electron scanning electron microscopy and confocal scanning light microscopy were conducted on polymethylmethacrylate (PMMA)-embedded medio-lateral slices. After maceration, scanning electron microscopy (SEM) was used to study the calcified cartilage surface in the 'wedges' intervening between the slices. An anatomically reproducible clustering of canals in the calcified cartilage was found at one site on the sagittal ridge in all the horses. The site is one that is relatively less loaded during joint function. These canals through calcified cartilage result from osteoclastic resorption (cutting cones) penetrating from bone through to the non-mineralized hyaline articular cartilage. Their presence may indicate a pathway for connection between bone and cartilage extracellular fluid. In one horse, repair of such canals by plugging with new calcified cartilage was demonstrated. Differences in the degree of mineralization of regions of cartilage were seen in the combined compositional-cum-topographical backscattered SEM images of the macerated 'tidemark' front. More-or-less circular patches of lower mineralization density were frequently centred on (and may possibly originate from) canals. These microanatomical features should be searched for in other joints, at other ages and in other species to discover their frequency and significance.

Key words articular calcified cartilage; backscattered electrons; canals through calcified cartilage; horse; scanning electron microscopy; subchondral bone.

Introduction

Much effort has been devoted to the study of the structure of calcified tissues in bones over several hierarchical scales between nanometres and centimetres. Much of this has been concentrated on the mineralization of physal cartilage that precedes its partial resorption and replacement by bone in the process of bone growth via endochondral ossification. An analogous sequence occurs in the deep layer of articular calcified cartilage in the younger animal. However, the rate of progress of

mineralization in articular cartilage slows so much in the established joint that it bears little similarity to that in growth plate cartilage. A layer of calcified cartilage 0.1–0.2 mm thick persists, but compared with our knowledge of the bounding hyaline cartilage and bone, information about this layer has not advanced much since Green et al. (1970) wrote that: 'Most accounts of osteoarthritis have it that the initial changes occur in the non-calcified part of the cartilage and disregard the calcified layer.'

The calcified cartilage is highly interdigitated with the bone, which attaches to its deep surface after piecemeal osteoclastic resorption. In older humans, such resorption frequently results in a complete penetration of calcified cartilage such that canals are generated which connect hyaline cartilage directly to the marrow space of the subchondral bone plate. Holmdahl & Ingelmark (1950) cite Petersen in the second edition of von Mollendorf's *Handbuch der mikroskopischen Anatomie des Menschen*

Correspondence

Professor Alan Boyde, Biophysics, Centre for Oral Growth and Development, St Barts and The London School of Medicine and Dentistry, Queen Mary, University of London, Turner Street, London E1 2AD, UK. E: a.boyde@qmul.ac.uk

Accepted for publication 24 September 2004

as describing such contact between marrow space and articular cartilage in humans: in referring to their own work in 10-month-old rabbits, they found isolated instances of 'offshoots of the medullary cavity reaching into the uncalcified articular cartilage', but their paper is largely concerned with marrow contact with the calcified layer only. In respect of human tissue (which they do not anywhere describe in their paper) they state that: 'In the human joints examined, there are small parts of the articular cartilages where we have not found any calcified cartilage. In these portions it is not unusual to find direct contact between the cartilage and the medullary cavity.'

Duncan et al. (1987) examined the human tibial plateau (age range 64–95 years) in both cadaveric and amputation samples, studying macerated material by secondary electron imaging in the scanning electron microscope (SEM). They showed canals which could be seen from the aspect of the tidemark mineralization front of the articular calcified cartilages which communicated with bone marrow space; these were also observed by Boyle & Jones (1983) in 'anorganic' preparations of aged human femoral heads. By histology, Duncan et al. (1987) showed that at least a proportion of such canals contained blood vessels. Oettmeier et al. (1989) also observed penetration of calcified cartilage in histology of aged human femoral heads from both fracture and osteoarthritis cases. Milz & Putz (1994) found, by microradiographic and histological study of samples of human tibiae from dissecting room cadavers aged 60–84 years, that there were spaces indicating direct contact between the marrow spaces of bone and the matrix of non-calcified, hyaline articular cartilage. They also surmised that the likely function of these spaces was to provide nutrition to the deep layers of the cartilage.

In humans, articular calcified cartilage is known to change during the development of osteoarthritis (Burr & Schaffler, 1997; Oegema et al. 1997). In the horse, it is known to change in exercise (Murray et al. 2001). Osteoarthritis and osteochondral fracture occur frequently in the metacarpophalangeal joint of wild horses (Cantley et al. 1999) and cause significant morbidity and wastage in competition horses (Johnson et al. 1994; Bailey et al. 1999). The incidence of canals that penetrate the calcified layer of articular cartilage has not, to our knowledge, been previously reported in the horse.

The 'Massey University Grass Exercise Study' (MUGES: Firth et al. 2000, 2004; Brama et al. 2000) constituted a

large whole-animal study of 2-year-old horses in early training to determine the response of various musculoskeletal tissues to a known amount of exercise. A marked increase in bone volume fraction (BVF: densification) in trabecular bone in the trained horses in this study has been documented by Boyle & Firth (2005) using quantitative backscattered electron (BSE) imaging. In conducting these higher resolution imaging studies of the subchondral epiphyseal bone of the distal aspect of the third metacarpal bone, we observed variability in the number and depth of resorption cavities in calcified cartilage, with infrequent spaces apparently traversing the entire calcified layer. In the present paper, we have exploited *en face* BSE scanning microscopy to observe the articular calcified cartilage mineralizing front morphology in greater detail. The results confirm that these spaces penetrate through the calcified layer to the non-calcified cartilage.

Materials and methods

We studied right distal third metacarpal segments from 14 2-year-old, female thoroughbred racehorses. After being paddock raised from birth until ~22 months, seven had been trained to race fitness over 14 weeks, and seven confined to 25 × 8-m grass yards (Firth et al. 2004). The density of intact bones had been studied by computed tomography (CT) and we performed microscopic studies to characterize the processes leading to the dramatic densification within trabecular bone (Boyle & Firth, 2005).

Distal third metacarpal samples were stored at –20 °C until sections were cut with a water-cooled, low-speed diamond saw. The bone sectioning plane was designed to focus on regions that the CT scans had shown to have changed as a consequence of training. The distal portion of the third metacarpal was first cut in the medio-lateral (frontal) plane in the line of the centre of the shaft to generate a 2–2.5-mm-thick, 60–65-mm-long by 50–55-mm-wide 'central' slice. Two further slices (1.5–2 mm thick) were cut perpendicular to the joint surface: a palmar piece inclined at 30–35° and a dorsal slice at 25° to the centre line, so as to pass through the rotation centre of the condyles (Fig. 1A). These slices, and transverse sections of the left distal third metacarpal from two horses, were embedded in polymethylmethacrylate (PMMA), and finished by diamond micromilling. The block faces were used for confocal scanning laser microscopy using oil-immersion

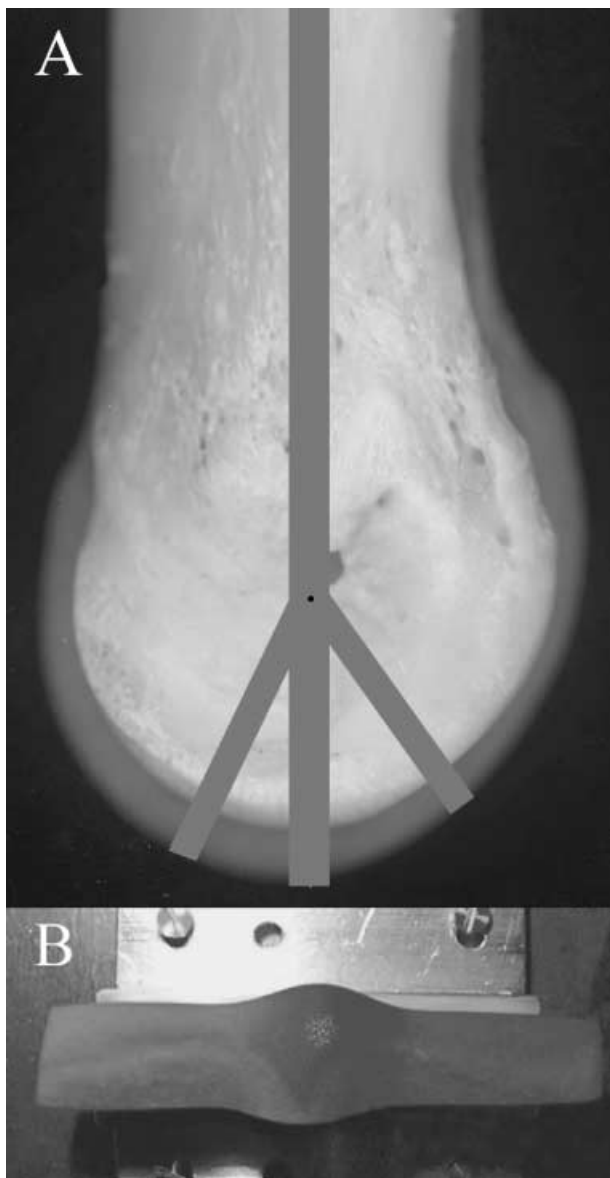


Fig. 1 (A) View of the medial side of the equine distal third metacarpal bone showing the location of the A, B and C slices for PMMA embedding and the intervening dorsal and palmar 'wedges' for maceration used in the present study. (B) Photograph showing a palmar wedge of horse 57 clamped ready for SEM study. The area where the highest incidence of clusters of penetrating canals was found is marked by a dotted overlay.

objectives and cover slipping with glycerine, which does not damage PMMA and can be removed with water. They were then carbon coated for SEM study.

To provide a broader view of the tidemark mineralization front with a good three-dimensional impression of its shape and complexity, we used the dorsal and palmar wedges left from the cutting process to make

unembedded SEM samples in which all cells and soft tissue elements had been removed so that we could study the tidemark mineral front *en face*. The wedges were prepared by treatment with a bacterial pronase detergent preparation (Tergazyme, Alconox Inc., New York, NY, USA; Boyde, 1984; Boyde & Jones, 1996) to remove all cells and unmineralized cartilage matrix, and were then washed, dried from ethanol and carbon coated from three principal directions (facing the two cut sides of each wedge and the natural tidemark surface), in each case tilting the sample through a wide range of angles to achieve complete coverage.

For scanning electron microscopy, both the macerated 'wedges' and the PMMA blocks were scanned using digital BSE imaging. The SEM used was a Zeiss DSM962 with IBAS external computer control (purchased from Zeiss UK Ltd, Welwyn Garden City, Herts., UK) with an annular solid-state BSE detector (KE Electronics Ltd, Toft, Cambs., UK).

Special clamping devices were made to support the wedges in the SEM so that the articular calcified cartilage mineralizing front and the two cut surfaces could be imaged at near-normal electron beam incidence, while still allowing tilting to achieve stereo and multi-tilt image sequences for display using motion parallax (Boyde, 2003: Fig. 1B). BSE imaging was used because this radically reduces electrostatic charging problems in the SEM. We generally used 30 kV to increase the BSE signal yield at the longer working distances needed to improve the depth of field. In the present case, BSE signal strength depends locally on morphology and composition and globally on distance from the detector. Thus the image contains both topographic and compositional information.

Such large pieces of porous bone tissue trap a vast amount of air and this is a major challenge for a turbo-molecular-pumped vacuum system. The difficulty was resolved by placing samples in the SEM chamber at the end of the working day, pumping down to the pressure at which the turbo-molecular pump was allowed to cut in, and then switching off overnight. In most cases, working conditions could be achieved after an additional 30 min to 1 h of pumping on resuming pumping the next day.

Results

The BSE SEM *en face* view of the tidemark mineralization front of the articular calcified cartilage demonstrated,

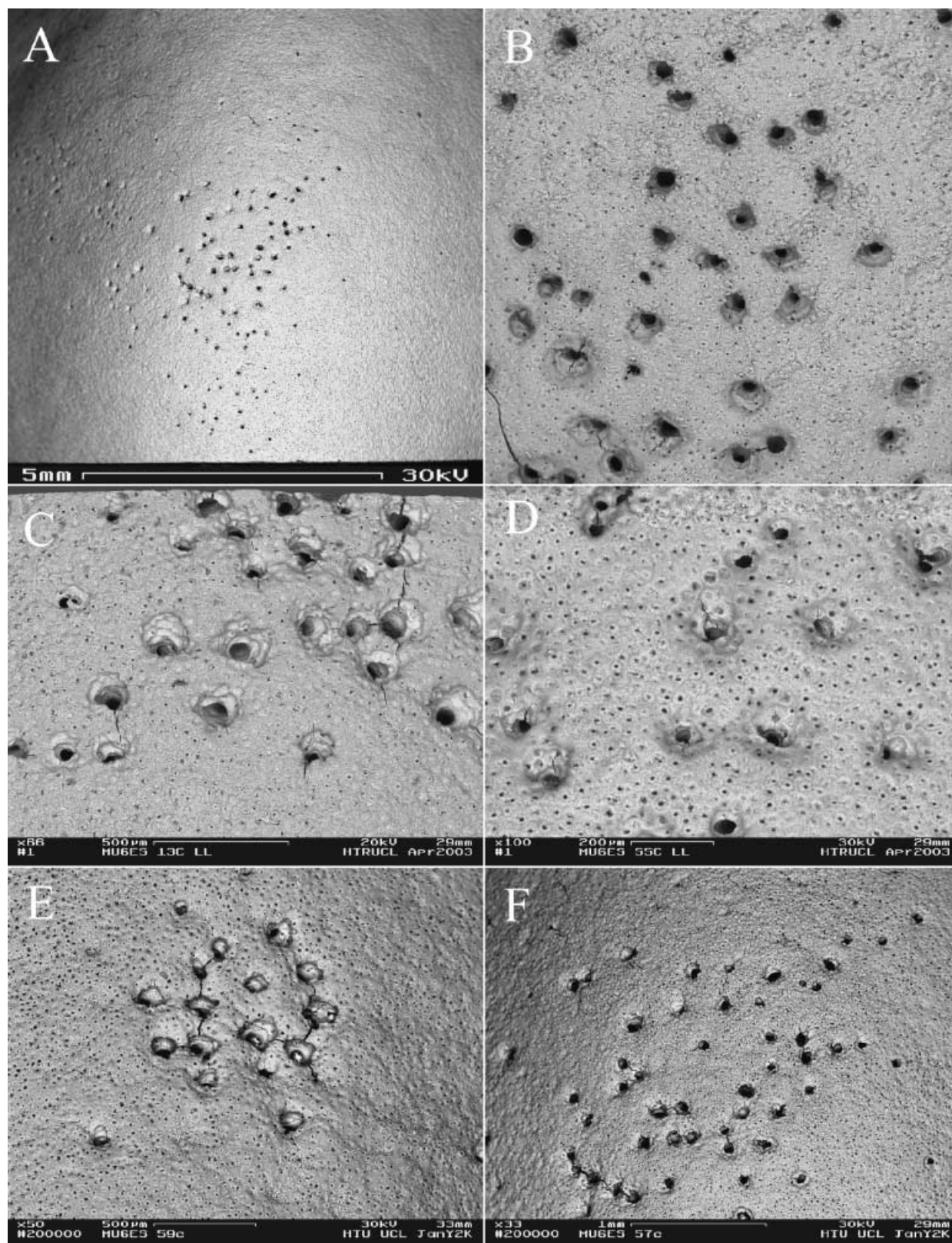


Fig. 2 BSE SEM images of calcified cartilage tidemark mineralization front (Tergazyme-cleaned, carbon-coated) surfaces in the median sagittal ridge of palmar wedges, showing clusters of penetrating canals just dorsal (anterior) to the transverse ridge. (A) Trained horse 57. (B) Control horse 25. Field width 1.782 mm. (C) Trained horse 13. (D) Trained horse 55. (E) Control horse 59: note linear grouping of canals. (F) Trained horse 57, again showing linear track grouping of canals.

Table 1 Counts of penetrating cartilage canals (foramina) at the calcified cartilage mineralizing front in distal third metacarpal wedges from 2-year-old thoroughbred racehorses. SR = median sagittal ridge. Other = sites excluding the sagittal ridge

Horse identifier	Dorsal SR	Palmar SR	Palmar other
Trained			
13	0	85	133
14	0	21	2
37	1	56	25
50	0	153	159
55	17	197	180
57	0	135	146
60	0	6	0
Control			
14PE	5	115	0
25	0	183	0
31	Missing	105	0
41	51	156	182
42	0	201	72
58	0	178	173
59	0	34	36

in all horses, clustering of penetrating canals at one site (indicated by the dotted patch at the centre of Fig. 1B), always on the palmar wedge just dorsal (anterior) to the point where the transverse ridge crosses the sagittal ridge (Fig. 1B).

In some horses, the distribution of the foramina was more widespread, extending further abaxially on the sagittal ridge and over the palmar portions of the medial and lateral condylar grooves. Foramina were counted to document that such canals could also be found sporadically at other sites (Table 1). Wide-field images were collaged into mega images, and canals were marked with a coloured spot using the eraser tool in Paint Shop Pro 5, counting the number of marks that were made. This prevented missing any, or recounting the same, foramina. The numbers showed a wide range between individuals. A Mann–Whitney test showed no significant difference ($P > 0.05$) between the trained and control groups. Table 1 quantifies the visually obvious difference between the dorsal and palmar sagittal ridge sites.

The diameters of these canals were between 50 and 200 μm . They were frequently wider at the calcified cartilage front (Fig. 2A–F). The canals had scalloped borders typical of osteoclastic resorption. In many instances, the foramina lined up in rows, suggesting that they arose as side branches of subchondral bone canals.

That the canals penetrated the thickness of the calcified cartilage from bone through into the non-mineralized cartilage was confirmed in the images of the PMMA-embedded slices (Fig. 3). BSE images do not show soft tissue histology, but this could be added by overlaying the confocal autofluorescence image of the tissue layer immediately beneath the block surface. This showed that hyaline cartilage was also resorbed (Fig. 3A,B).

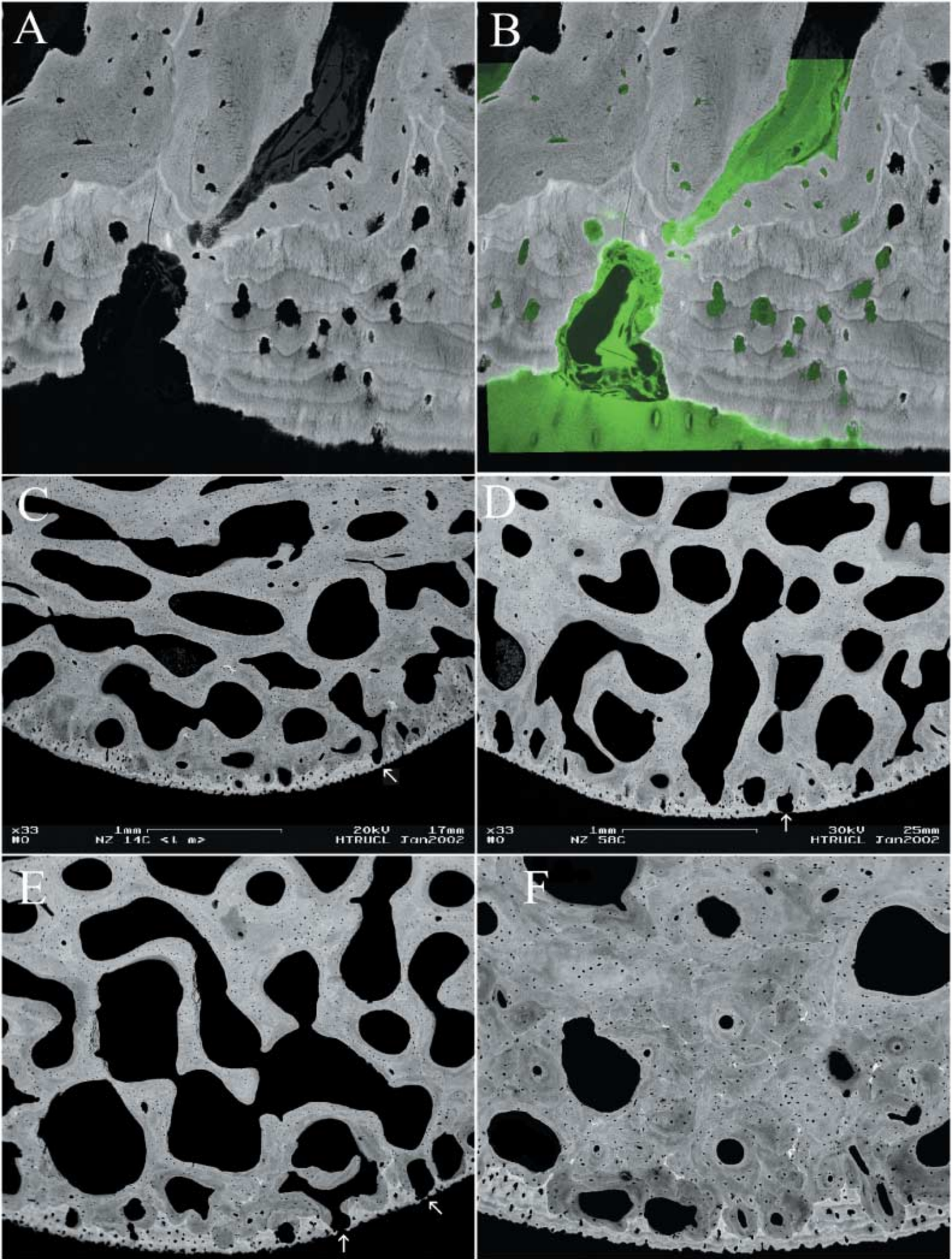
The volume density of subchondral bone in the sagittal ridge is low, such that there are large marrow spaces close to calcified cartilage from which the penetrating canals may arise (Fig. 3C–F).

Differences in the degree of mineralization of the mineralization front 'surface' (NB: it is only a surface in our contrived samples) layer of calcified cartilage could be seen in the wider field *en face* BSE images (Fig. 4A–C). More-or-less circular patches of lower mineralization density frequently appeared to be centred on canals where calcified cartilage had been penetrated. This broader context information could be distinguished from local signal modulation due to topography and to local differences in calcification. The present studies confirmed findings in other mammalian species in showing locally advanced mineralization and higher degrees of mineralization next to chondrocyte lacunae at the mineralizing front (Fig. 2D–F: Boyde & Jones, 1983).

Repair of the canals by plugging with new cartilage that proceeded to calcify was found in one horse (Fig. 4D,E). Histology confirmed that the tissue was new, and was cartilage. It contained large and separated lacunae, as against the clustered lacunar groups (sometimes called chondrons) of the deep layers of the hyaline cartilage, which have an orientation perpendicular to the cartilage surface. The repair tissue also had a substantially lower degree of mineralization, and the perilacunar hypermineralization (Fig. 2D–F: Boyde & Jones, 1983) characteristic of the original calcified cartilage was lacking.

Discussion

Osteoclastic resorption events normally lead to tunnel-wise partial removal of the deeper layers of the calcified cartilage, such that, when the process is reversed, the newly apposed subchondral bone is intimately attached. Here we report the regular complete penetration of calcified cartilage, such that osteoclasts breach into soft cartilage. We conclude that this process is normal, since it was found in a confined anatomical distribution



in every horse we studied. Nevertheless, this penetrative process was also found in other regions of the distal third metacarpal bones in some of the horses.

The main canal cluster site was just dorsal to the so-called transverse ridge on the distal articular surface of the third metacarpal. This ridge is directly opposite the ligamentous attachment of the proximal sesamoid bones and the proximo-palmar aspect of the proximal phalanx, when the horse is in the normal standing position, i.e. in the region where there is no direct abutment of cartilage of either the proximal sesamoid bone or the proximal phalanx against that of the third metacarpal. Joint surface stresses on the median sagittal ridge are unknown, but it is likely that this is a relatively low-loaded site. Subchondrally, it generally shows a more open trabecular pattern (e.g. Boyde et al. 1999), even in horses that have been trained for long periods of time. The concentration of canals penetrating the calcified cartilage might suggest a pathway for connection between extracellular fluid in bone and hyaline cartilage. Their presence certainly indicates that the matrix-degrading enzymes produced by osteoclasts were in direct contact with unmineralized cartilage, and Clark (1990) showed removal of intercollagenous, ground substance matrix components in SEM images of freeze fracture preparations through human knee joint cartilage.

This is the first report documenting the presence and the localized distribution of canals penetrating calcified cartilage in normal, young large mammals. In aged human knee and hip joints, several authors have shown that some of these resorptive events lead to a complete penetration of the calcified layer, such that bone marrow space is in direct contact with uncalcified, hyaline articular cartilage (Boyde & Jones, 1983; Duncan et al. 1987; Milz & Putz, 1994). Holmdahl & Ingelmark (1950) noted that this also occurs infrequently in young mature rabbits.

In the newborn foal, all epiphyses are ossified, but not fully. Until the bony epiphysis is expanded by endochondral ossification, and the 'subchondral plate'

forms, vascular elements course through the as yet unossified epiphyseal cartilage up to, but not into, the articular cartilage proper. The age at which the horse is said to be mature is 4–5 years, but this is an indication of when total growth, measured in terms of height, no longer increases. The exact time at which the distal third metacarpal epiphysis ceases to grow has not been investigated. Certainly there is little growth here after 18 months of age, and it would be surprising if the canals we have observed are morphologically or functionally related to the vascular structures easily observed in third metacarpal cartilage in foals of much younger age (Firth & Poulos, 1993).

The canals were usually concentrated in sites that were not those where cartilage surface stress would be expected to be highest. It cannot be assumed that training exercise results in imposition of higher stress in all sites on cartilage surfaces. The median sagittal ridge does not appear to increase its bone volume fraction in trained horses (Boyde & Firth, 2005), and bone mineral content determined by CT can reduce in some parts of the epiphyseal bone while increasing in others, as a result of training (Firth et al. 1999, 2000). Further study of the whole joint surface is required to allow mechanistic hypotheses to be formulated.

In all bones studied, our attention has been attracted by large variations in the degree of mineralization within calcified cartilage, which are clearly detectable with the sensitivity and resolution of quantitative BSE imaging. It is clear that the 'multiple tidemarks' of decalcified tissue histology reflect stratification in the degree of mineralization. Far from being 'pathological', this is the normal situation, and it relates to the detection of patches of varying density in the *en face* BSE images of the mineral front of the calcified cartilage. Mineralization levels will be lower when mineralization recommences after a resting phase at the calcified cartilage mineralizing front. We propose that the low-density patches represent a kind of 'wave' of

Fig. 3 BSE SEM images of the median sagittal ridge in micromilled, PMMA-embedded transverse sections. (A) Control horse 14PE showing a single penetrating canal. Field width 445 μm . (B) The same field with a confocal fluorescence image overlaid. Note that hyaline cartilage matrix has been resorbed. (C) The dorsal face of palmar oblique section C of trained horse 14: a single canal nearly penetrates the calcified cartilage at the arrow. Note the preferred horizontal-transverse orientation of the large subchondral bone marrow spaces (black). (D) The dorsal face of palmar oblique section C of control horse 58 showing a single penetrating canal at the arrow. Note the vertical orientation of the central large marrow space (black). (E) The dorsal face of palmar oblique section C of control horse 41 showing a penetrating canal at the vertical arrow and one which nearly penetrates the calcified cartilage at the oblique arrow. Note large marrow spaces (black). (F) The dorsal face of palmar oblique section C of control horse 58. Note the lower volume fraction of marrow spaces (black) compared with Fig. 3(C–E) and evidence of high turnover, with interstitial lamellar patches left over from past, frequent turnover events. Field width 1.35 mm.

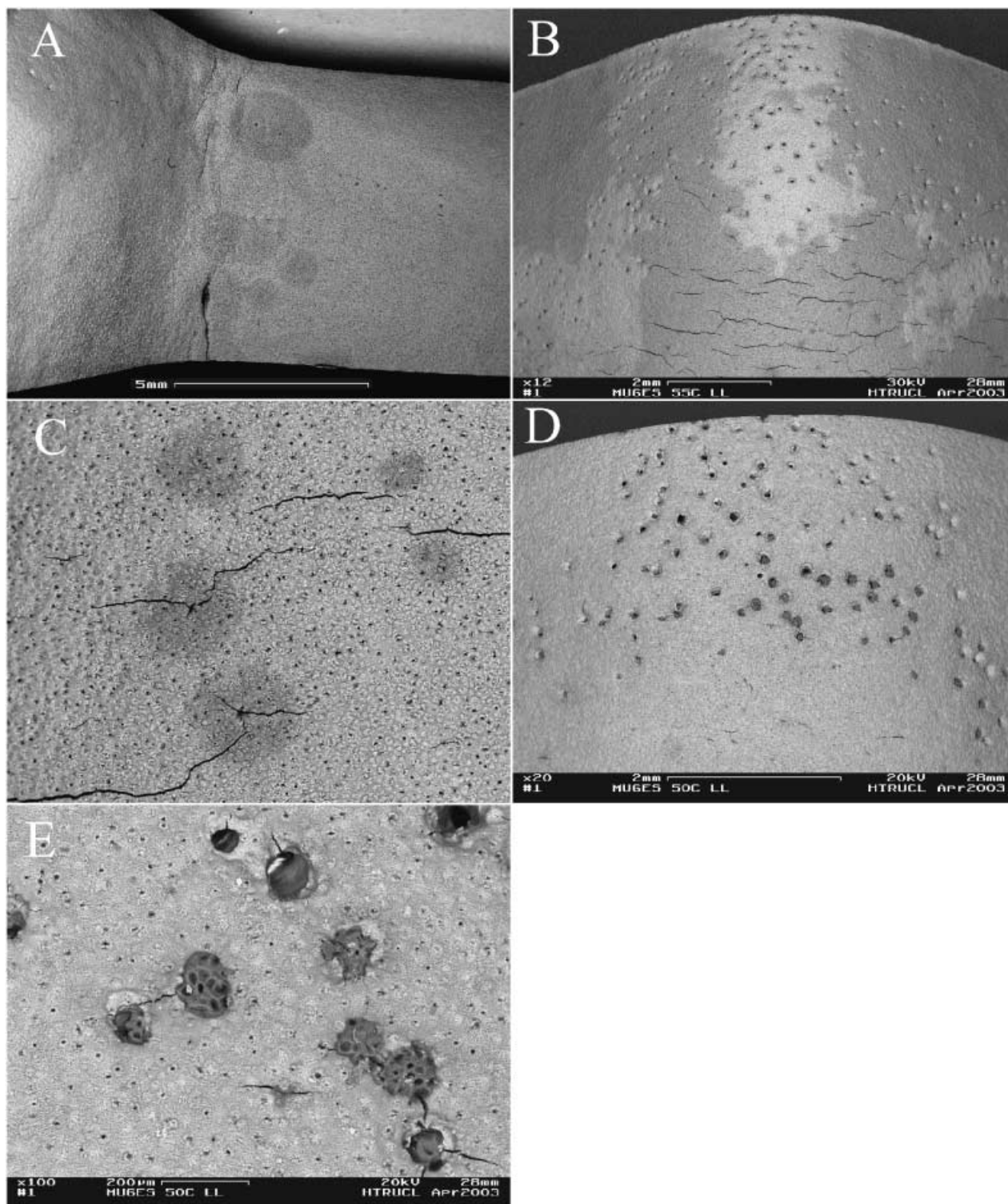


Fig. 4 BSE SEM images of calcified cartilage mineralizing front surfaces in Tergazyme-cleaned palmar wedges. (A) The medial condylar groove of control horse 59 showing a deep crack or cleft in the palmar aspect and several patches of surface which are darker, indicating a lower level of mineralization of the calcified cartilage: some of these are centred on penetrating canals. (B) The sagittal ridge of control horse 59. Note lighter and darker patches of surface, indicating different levels of mineralization. (C) The sagittal ridge of trained horse 14 showing darker patches, mostly centred on penetrating canals, indicating a lower level of mineralization of the surface. Field width 1.782 mm. (D,E) The median sagittal ridge in the palmar wedge of trained horse 50 showing the usual cluster of penetrating canals: several canals are plugged with reparative calcified cartilage having a lower degree of mineralization than the surrounding, original calcified cartilage.

progression of the initiation of new calcification across the 'tidemark'. It is of great interest that patches of lower mineralization density frequently appeared to be centred on, and thus probably start from, the sites of canals where calcified cartilage had been penetrated.

We also find large variations in the thickness and in the structural features of calcified cartilage, but we have not yet determined the extent to which these may be related to the local remodelling history of the underlying SCB (Sub Chondral Bone). It might be anticipated that high-turnover, low-density bone would be associated with thinner calcified cartilage because 'cutting cones' enter and remove calcified cartilage. This point deserves further investigation.

The phenomenon of the foramina lining up in rows can be explained if they arise as side branches of the same subchondral bone canals. It is probable that clustering of cutting cone events is probably a general phenomenon in bone (Bell et al. 2001).

The procedure for combining confocal autofluorescence imaging of the block surface layer with BSE SEM imaging has been of particular value in this study. With the benefit of hindsight, we now regret that we did not use standard fixation protocols to obtain better cellular preservation, but this development was not foreseen when we took the tissue, when our aim was to preserve tissue calcification above all else.

Our findings also address the issue of repair of the penetrating foramina. The tidemark mineralization front is locally removed, and if the canal is to be plugged with calcified cartilage, it may first have to be filled with new hyaline cartilage. Here we show that the new tissue resembles the repair cartilage tissue seen in experimental studies of joint cartilage repair (Smith et al. 2003). It lacks chondrocytic lacunar clusters, it has a substantially lower degree of mineralization and it lacks the perilacunar hypermineralization (Boyde & Jones, 1983) that typifies the progress of the original calcified cartilage mineralizing front. That the canals do repair is in itself of considerable significance.

The formation of the canals raises the question of whether the penetration of osteoclastic proteolytic enzymes into deep hyaline cartilage is an undesirable and accidental by-product of the normal processes whereby bone attaches itself to articular cartilage. This process has to occur in order to limit the thickness which is reached by the calcified cartilage layer that has to attach and to mediate between the mechanical functions of soft cartilage and hard bone.

Acknowledgements

The Massey University Grass Exercise Study was funded by the New Zealand Equine Research Foundation and the Foundation for Research, Science and Technology (NZ). This work was supported by the Horserace Betting Levy Board in the Department of Anatomy and Developmental Biology at University College London (UCL), where Roy Radcliffe and Maureen Arora provided valuable technical assistance. The automated digital SEM was funded by the MRC (UK).

References

- Bailey CJ, Reid SW, Hodgson DR, Rose RJ (1999) Impact of injuries and disease on a cohort of two- and three-year-old Thoroughbreds in training. *Vet. Rec.* **145**, 487–493.
- Bell KL, Loveridge N, Reeve J, Thomas CD, Feik SA, Clement JG (2001) Super-osteons (remodeling clusters) in the cortex of the femoral shaft: influence of age and gender. *Anat. Rec.* **264**, 378–386.
- Boyde A, Jones SJ (1983) Scanning electron microscopy of cartilage. In *Cartilage, Vol. I Structure, Function and Biochemistry* (ed. Hall BK), pp. 105–148. New York: Academic Press.
- Boyde A (1984) Methodology of calcified tissue specimen preparation for scanning electron microscopy. In *Methods of Calcified Tissue Preparation* (ed. Dickson GR), pp. 251–307. Amsterdam: Elsevier.
- Boyde A, Jones SJ (1996) SEM of bone: instrument, specimen and issues. *Microsc. Res. Techn.* **33**, 92–120.
- Boyde A, Haroon Y, Riggs CM (1999) Three dimensional structure of the distal condyles of the third metacarpal bone. *Equine Vet. J.* **31**, 122–129.
- Boyde A (2003) Improved digital SEM of cancellous bone: scanning direction of detection, through focus for in-focus and sample orientation. *J. Anat.* **202**, 183–194.
- Boyde A, Firth EC (2005) Musculoskeletal responses of two year old Thoroughbreds in training: quantitative backscattered electron SEM and confocal fluorescence microscopy of the epiphysis of the third metacarpal bone. *NZ Vet. J.* in press.
- Brama PA, Tekoppele JM, Bank RA, Barneveld A, Firth EC, Van Weeren PR (2000) The influence of strenuous exercise on collagen characteristics of articular cartilage in Thoroughbreds age 2 years. *Equine Vet. J.* **32**, 551–554.
- Burr DB, Schaffler MB (1997) The involvement of subchondral mineralized tissues in osteoarthritis: quantitative microscopic evidence. *Microsc. Res. Techn.* **37**, 343–357.
- Cantley CE, Firth EC, Delahunt JW, Pfeiffer DU, Thompson KG (1999) Naturally occurring osteoarthritis in the metacarpophalangeal joints of wild horses. *Equine Vet. J.* **31**, 73–81.
- Clark JM (1990) The structure of vascular channels in the subchondral plate. *J. Anat.* **171**, 105–115.
- Duncan H, Jundt J, Riddle JM, Pitchford W, Christopherson T (1987) The tibial subchondral plate. *J. Bone Joint Surg.* **69A**, 1212–1220.

- Firth EC, Poulos PW** (1993) Vascular characteristics of the cartilage and subchondral bone of the distal radial epiphysis of the young foal. *NZ Vet. J.* **41**, 73–77.
- Firth EC, Delahunt J, Wichtel JW, Birch HL, Goodship AE** (1999) Galloping exercise induces regional changes in bone density within the third and radial carpal bones of Thoroughbred horses. *Equine Vet. J.* **31**, 111–115.
- Firth EC, Rogers CW, Jopson N** (2000) Effects of racetrack exercise on third metacarpal and carpal bone of New Zealand thoroughbred horses. *J. Musculoskel. Neuronal Interact.* **1**, 145–147.
- Firth EC, Rogers CW, Perkins NR, Anderson BH, Grace ND** (2004) Musculoskeletal responses of two year old thoroughbred horses to early training. 1. Study design, and clinical, nutritional, radiological, and histological observations. *NZ Vet. J.* in press.
- Green WT, Martin GN, Eanes ED, Sokoloff L** (1970) Microradiographic study of the calcified layer or articular cartilage. *Arch. Pathol.* **90**, 151–158.
- Holmdahl DE, Ingelmark BE** (1950) The contact between the articular cartilage and the medullary cavities of the bone. *Acta Ortho. Scand.* **20**, 156–165.
- Johnson BJ, Stover SM, Daft BM, et al.** (1994) Causes of death in racehorses over a 2-year period. *Equine Vet. J.* **26**, 327–330.
- Milz S, Putz R** (1994) Lückenbildungen der subchondralen Mineralisierungszone des Tibialplateaus. *Osteologie* **3**, 110–118.
- Murray RC, Vedi S, Birch HL, Lakhani KH, Goodship AE** (2001) Subchondral bone thickness, hardness and remodelling are influenced by short-term exercise in a site-specific manner. *J. Orthop. Res.* **19**, 1035–1042.
- Oegema TR, Carpenter RJ, Hofmeister F, Thompson RC** (1997) The interaction of the zone of calcified cartilage and subchondral bone in osteoarthritis. *Microsc. Res. Techn.* **37**, 324–332.
- Oettmeier B, Abendroth K, Oettmeier S** (1989) Analyses of the tidemark on human femoral heads. II. Tidemark changes in osteoarthrosis – A histological and histomorphometric study in non-decalcified preparations. *Acta Morphol. Hungarica* **37**, 169–180.
- Smith GD, Richardson JB, Brittberg M, et al.** (2003) Autologous chondrocyte implantation and osteochondral cylinder transplantation in cartilage repair of the knee joint. *J. Bone Joint Surg.* **85A**, 2487–2488.